

Contract No.:

This manuscript has been authored by Battelle Savannah River Alliance (BSRA), LLC under Contract No. 89303321CEM000080 with the U.S. Department of Energy (DOE) Office of Environmental Management (EM).

Disclaimer:

The United States Government retains and the publisher, by accepting this article for publication, acknowledges that the United States Government retains a non-exclusive, paid-up, irrevocable, worldwide license to publish or reproduce the published form of this work, or allow others to do so, for United States Government purposes.

Isotopic Signatures of Lithium Carbonate and Lithium Hydroxide Monohydrate Measured Using Raman Spectroscopy

Willis B. Jones, Jason R. Darvin, K. Alicia Strange Fessler*, Patrick E. O'Rourke

Savannah River National Laboratory, Aiken, SC 29803, United States

*Corresponding Author. email: alicia.fessler@srnl.doe.gov, mailing address: 301 Gateway Dr, Aiken, SC 29803

Abstract

Lithium isotopic ratios have wide ranging applications as chemical signatures, including improved understanding of geochemical processes and battery development. Measurement of isotope ratios using optical spectroscopies would provide an alternative to traditional mass spectrometric methods, which are expensive and often limited to a chemical laboratory. Raman spectra of ${}^7\text{Li}_2\text{CO}_3$, ${}^6\text{Li}_2\text{CO}_3$, ${}^7\text{LiOH}\cdot\text{H}_2\text{O}$ and ${}^6\text{LiOH}\cdot\text{H}_2\text{O}$ have been measured to determine the effect of lithium isotope substitution on the Raman molecular vibrations. Thirteen peaks were observed in the spectrum of lithium carbonate, with discernable isotopic shifts occurring in eleven of the thirteen vibrations, two of which have not been previously reported in the literature. The spectrum of lithium hydroxide monohydrate contained nine peaks, with discernable isotopic shifts occurring in eight of the nine vibrations, four of which have not been previously reported in the literature. The Raman spectral data reported here for lithium carbonate and lithium hydroxide monohydrate are in agreement with the previously reported works in the literature, in which the Raman active modes of these molecules were first identified and assigned. However, due to the stability and resolution of the detection system used in this work, isotopic shifts with a magnitude less than one wavenumber have been identified. Principal Component Regression was used to evaluate the sensitivity to isotopic content of small Raman peak shifts in Li_2CO_3 and indicates that differences greater than 2 atom-% could be reliably determined. These measurements add to the body of work on Li isotope Raman spectroscopy for these two compounds and increases the number of Raman bands which could be used for lithium isotope content analysis.

Keywords: Raman spectroscopy, isotope, lithium

Introduction

Lithium isotopic ratios are important chemical signatures that have applications in geochemistry and battery development. In the world of geochemistry, lithium isotope ratios measured in both fresh and seawater have been shown to be dependent on the environment in which the water is sampled.

Hyperfiltration of groundwater through subterranean clay membranes leads to significant lithium fractionation, which in turn can lead to groundwater sampling that is not chemically or isotopically representative.¹ Similarly, lithium isotopes in minerals derived from magmatic melting processes can differ significantly from their source minerals.² Fractionation of lithium isotopes in minerals is dependent upon the length of Li-O bonds and also by the Li coordination number.³ Geothermal reservoirs can be characterized using multi-species isotopic analysis, and lithium specifically is subject to mass dependent fractionation directly related to geological parameters such as depth and temperature.⁴ The ⁶Li isotope has been shown to leach from minerals before ⁷Li as rocks dissolve.⁵ Low temperature weathering processes on the seafloor have been shown to preferentially remove the ⁷Li isotope from seawater.⁶

Lithium isotopic ratios also play an important part in the improvement of lithium ion batteries. Lithium cobalt oxide (LiCoO₂), one of the most common cathode materials in lithium ion batteries, has been shown to preferentially release the ⁷Li isotope into electrolytes.⁷ In contrast, lithium manganese oxide (LiMn₂O₄), a common alternative cathode material, was found to preferentially release the ⁶Li isotope.⁸ Graphite anodes have been shown to preferentially uptake the ⁶Li isotope from organic electrolytes.⁹ Thus, the isotope ratios of lithium compounds used as cathodes in batteries could be optimized to improve battery efficiency, depending on interactions with the electrolytes and anodes used in the electrochemical system.

Measurement of lithium isotope ratios also has applications in reagent characterization, which is important when procuring chemicals that are to be used for isotopic standards. An analysis of commercially available lithium containing reagents revealed that over 15% of the examined compounds were depleted in the ^6Li isotope.¹⁰

Currently there are limited techniques available for rapid field analysis of lithium isotope ratios. Isotopic analyses are typically performed using mass spectrometric methods. Such methods are extremely sensitive but often prohibitively expensive, not easily portable, and largely limited to implementation in a chemical laboratory. Building an understanding of the isotopic detection capabilities of various optical spectroscopic techniques would provide the scientific basis for developing a standalone system capable of making isotopic measurements in a more portable and affordable fashion. Laser-induced breakdown spectroscopy (LIBS) has been demonstrated as a useful tool for measuring the isotopic shifts in the atomic spectrum of lithium.¹¹ The isotopic shifts in atomic spectra are on the order of tens of picometers or less and require a high-resolution spectrometer to resolve, which tend to be large or cover a small spectral range. LIBS is a destructive technique and may not be ideal when further analysis needs to be performed or sample preservation is important. In this work, Raman spectroscopy was investigated as a possible spectroscopic technique to distinguish Li isotopes present in samples due to the larger spectral peak shifts observed for isotopic substitutions in molecular spectra (on the order of a wavenumber or larger) and the non-destructive nature of the technique.

Raman spectroscopy is a molecular optical technique that offers uniquely characteristic spectra for Raman-active compounds. Raman spectroscopy can also provide isotopic information if a particular molecular vibration involves the isotope of interest, as the frequency of a molecular vibration is proportional to the reduced mass of the atoms involved in the vibration.¹² Thus, the substitution of a low mass atom for an isotope of a higher mass reduces the frequency at which a molecular vibration occurs. Raman measurements of lithium hydroxide,¹³⁻¹⁴ lithium hydroxide monohydrate,¹⁴⁻¹⁵ lithium

oxide,¹⁶ lithium carbonate,¹⁷⁻¹⁸ and lithium hydride¹⁹ have been demonstrated in the literature, but the effects of lithium isotope substitution on the Raman spectra have not been thoroughly investigated. Some lithium isotopic shifts in the Raman spectra of Li_2CO_3 and $\text{LiOH}\cdot\text{H}_2\text{O}$ have been previously described in the literature,²⁰⁻²² and this work expands on those results. While this manuscript is largely focused on the identification of new isotopic shifts in the spectra of pure Li_2CO_3 and $\text{LiOH}\cdot\text{H}_2\text{O}$, it is important to note that real samples or mixtures would likely contain a significantly lower amount of lithium compounds. Thus a sample purification or extraction step would be necessary to accurately determine the isotope ratios in real samples using Raman spectroscopy, which traditionally struggles with sensitivity.

Materials and experimental methods

Pressed pellets of $^6\text{Li}_2\text{CO}_3$, $^7\text{Li}_2\text{CO}_3$, $^6\text{LiOH}\cdot\text{H}_2\text{O}$, and $^7\text{LiOH}\cdot\text{H}_2\text{O}$ were prepared from their powdered forms. Assays of the as received material indicate the ^6Li sample was 95 atom% ^6Li and the ^7Li sample was 99 atom% ^7Li . It is assumed the remaining Li content is the other isotope. The pellets were sealed in glass vials under argon atmosphere to prevent absorption of water from the air. A diagram of the experimental system is provided in Fig. 1. Sample pellets were analyzed inside of the vials using a 785 nm laser. The laser passed through a laser line filter and was focused into the sample vials using a planoconvex lens. Scattered light was collected, passed through a 785 nm longpass filter, and focused onto a fiber optic using a second planoconvex lens. The fiber optic directs the remaining Raman scattered light into a Horiba iHR320 spectrometer, which is equipped with three gratings. Spectrometer and detector settings were computer controlled using a software suite built at Savannah River National Laboratory. The highest resolution grating available (1800 grooves/mm) was used during the collection of Raman spectra. Due to the use of the high resolution grating, spectral collection across a series of wavelength regions was required to obtain full range Raman spectra. The wavelength region was initially centered at 800 nm and increased in 20 nm increments to a final window centered at 860 nm. No peaks

were observed above the 860 nm wavelength window due to the poor performance of both the grating and detector at higher wavelengths. All spectra were collected in triplicate in each wavelength window using a 30 second integration time. The three spectra were hot pixel and gamma ray corrected, then averaged. All observed peaks in the Raman spectra were fit with a Voigt profile using OriginPro software. Peak locations reported in the following results sections are the center of the fit Voigt profiles.

Studies to evaluate the sensitivity of isotopic determination to small shifts in the Raman spectra of Li_2CO_3 were conducted using the same spectrometer and detector as above but used 532nm excitation and an Ondax THz-Raman fiber optic probe. Samples used in the sensitivity study were prepared by grinding with mortar and pestle, and pouring the powder into disposable plastic cuvettes.

[Insert Figure 1]

Results and Discussion

Spectrometer Reproducibility

To demonstrate instrument reproducibility, the spectrometer and detector system were calibrated for consistency by altering the spectrometer settings and taking a series of measurements on the lithium carbonate pellets. After taking an initial set of spectra for a background correction, the reported Raman spectra of each carbonate pellet were recorded after moving the sample pellets, switching wavelength regions on the 1800 lines/mm grating, and switching between different gratings. The results of altering the detector system parameters on two bands observed in the Raman spectra of $^7\text{Li}_2\text{CO}_3$ are displayed in Fig. 2A. No shifts in the Raman bands were observed upon changing any spectrometer settings or switching the sample pellet. The change in the intensity of the continuum background observed throughout the subsequent measurements is a result of movement of the sample pellet, which was manually positioned in the laser path.

A comparison between the Raman spectra of the lithium carbonate samples containing ^6Li and ^7Li isotopes indicates a small shift of the Raman bands centered at 101 and 132 cm^{-1} , as shown in Fig. 2B. The shifts observed in wavenumber are quite small, only on the order of 1 cm^{-1} for the band at 101 cm^{-1} . The spectra shown in Fig. 2B were recorded after movement of the sample pellets only. The spectrometer settings were unchanged during the measurement of the Raman spectra of the two pellets. Due to the demonstrated reproducibility of the instrument and experimental setup, even if the detector settings had been altered in between measurements, the shifts in the bands are undoubtedly caused by the lithium isotope present in the sample pellet and not a result of changes in the spectrometer settings. Peak locations for both isotopically substituted lithium carbonate pellets and wavenumber shifts caused by changing experimental parameters are provided in Table 1. The largest band shift calculated when spectrometer parameters were altered (approximately 0.1 cm^{-1}) is below the resolution per pixel at 100 cm^{-1} (approximately 0.22 cm^{-1} as shown in Tables 2 and 3). All of the other shifts observed in wavenumber after the change of the spectrometer parameters are significantly smaller than 0.1 cm^{-1} (around 0.05 cm^{-1} or lower). The peak locations reported in Table 1 were calculated by a fitting operation using a Voigt profile, but in all the measurements made for a given sample pellet the maximum peak intensity on the detector was on the exact same pixel when moving the sample pellet and switching the detector parameters. The 0.4 cm^{-1} shift of the 101 cm^{-1} peak observed when comparing the $^6\text{Li}_2\text{CO}_3$ and $^7\text{Li}_2\text{CO}_3$ pellets has a shift on the detector of 2 pixels for the maximum peak intensity. Therefore, the peak shifts were concluded to be from isotope-substitution and no other source.

[Insert Figure 2]

Table 1. The locations of the Raman bands observed for two lithium carbonate vibrations after switching measurement parameters. The shifts provided are relative to the initial measurement for each pellet.

Measurement	^7Li Peak Locations (cm^{-1})				^6Li Peak Locations (cm^{-1})			
	Band	Shift	Band	Shift	Band	Shift	Band	Shift
initial measurement	101.20	--	132.32	--	101.63	--	133.77	--

switching pellets	101.22	0.02	132.35	0.03	101.61	-0.02	133.78	0.01
switching wavelengths	101.15	-0.05	132.29	-0.03	101.53	-0.10	133.69	-0.08
switching gratings	101.22	0.02	132.37	0.05	101.61	-0.02	133.77	0.00

Lithium carbonate bands

Raman spectra obtained for isotopically substituted lithium carbonate are provided in Fig. 3. All of the peaks observed in the Raman spectra of lithium carbonate have been previously identified in the literature.^{18,20-21} Peak assignments and observed isotopic shifts are provided in Table 2. Two new isotopic shifts in the Raman spectrum of lithium carbonate have been identified, as well as experimental evidence that several other Raman band shifts previously reported are due to the substitution of the lithium isotope

Thirteen peaks were observed in the Raman spectrum of lithium carbonate in this work, which agreed well with literature values. Six of these peaks at low shift values (below 350 cm⁻¹), correspond to rotational and translational vibrations of the carbonate ion in the lattice structure.²⁰ Five of the six vibrations exhibit very slight isotopic shifts (on the order of 1 cm⁻¹) due to substitution of the lithium atom even though the vibration does not directly involve the lithium, as shown in Fig. 3A. These five isotopic shifts were also observed by Hase but were not attributed to lithium substitution specifically.²⁰ Prior research has demonstrated cation substitution in minerals can cause peak shifts in Raman active vibrations not directly involved with the cation.²³⁻²⁴ It follows logically that isotopic substitution should produce similar shifts, albeit at much smaller magnitudes, because the mass discrepancy between two isotopes of one element is typically much smaller than the mass difference caused by substituting one element for another. The references provided observe shifts upon substituting magnesium with iron, which is a mass increase on the order of 200%.²³⁻²⁴ Lithium is one of the lightest elements, and as such exhibits one of the biggest relative isotopic mass differences, but the mass increase of ⁷Li when

compared to ^6Li is only 17%. This small mass difference could explain the small shifts observed upon lithium isotope substitution for non-lithium involved vibrations.

Four peaks in the middle frequency region of the spectrum are attributed to translational lattice vibrations of Li-O groups and exhibit significant isotopic shifts on the order of 25 cm^{-1} , as shown in Fig. 3B. These four isotopic shifts were also observed by Hase.²¹ Two Raman bands arising from the ν_4 fundamental vibration of the CO_3 group (A_g+B_g Raman modes) exhibit small isotopic shifts below 1 cm^{-1} , as shown in Fig. 3C. The isotopic shifts of these bands are difficult to discern due to the relatively broad nature of the peaks and have not yet been reported in the literature. The Raman bands arising from these vibrations are relatively weak and noisy due to the poor performance of both the grating and detector at longer wavelengths. To further clarify the isotopic shifts, the spectra shown in Fig. 3C were subjected to a five point rolling average and plotted with the calculated Voigt profiles, as shown in Fig. 4. The calculated Voigt model fits the bands well, and the Raman bands exhibit isotopic shifts of a magnitude less than 1 cm^{-1} . The peak observed near 1090 cm^{-1} in the Raman spectrum of lithium carbonate (see Fig. 3D) is attributed to a symmetric bond stretching of the carbonate ion, which does not exhibit any shift upon substitution of the lithium isotope.

[Insert Figure 3]

[Insert Figure 4]

Table 2. The shifts observed in the Raman bands of lithium carbonate upon substitution of ^6Li and ^7Li isotopes. The band assignments are based on the literature.

Raman band locations (cm^{-1}) ^{17,20-21}			Observed band locations and shifts (cm^{-1}) in this work				Assignments to the lattice vibrations ^{17-18,20-21}
^6Li	^7Li	Strength	^6Li	^7Li	Shift / #pixels	Resolution per pixel	
99	97	VS	101.62	101.24	0.38 / 2	0.22	CO_3 translation/ rotation
130	128	M	133.73	132.33	1.40 / 6	0.22	CO_3 translation/ rotation
160	157	S	163.40	161.87	1.53 / 7	0.21	CO_3 translation/ rotation
196	192	S	200.18	198.76	1.42 / 7	0.21	CO_3 translation/ rotation
220	220	VW	223.81	223.91	-0.10 / < 1	0.21	CO_3 translation/ rotation
277	275	W	279.26	278.73	0.53 / 3	0.20	CO_3 translation/ rotation

402	375	VW	404.69	379.77	24.92 / 125	0.20	Li-O translation
459	433	VW	464.84	436.51	28.33 / 142	0.20	Li-O translation
518	486	VW	523.44	491.61	31.83 / 168	0.19	Li-O translation
547	513	VW	552.34	517.11	35.23 / 185	0.19	Li-O translation
n.s.	712	n.s.	716.12	715.60	0.52 / 3	0.18	V ₄ fundamental of CO ₃
n.s.	747	n.s.	753.57	752.70	0.87 / 5	0.18	V ₄ fundamental of CO ₃
n.s.	893	n.s.	n.o.	n.o.	n.o.		B _g Raman mode
n.s.	1091	n.s.	1095.82	1095.74	0.08 / < 1	0.15	Symmetric CO ₃ stretch

n.s. – not studied, n.o. – not observed, VS – very strong, S – strong, M – medium, W – weak, VW – very weak

Lithium hydroxide monohydrate bands

Raman spectra obtained for isotopically substituted lithium hydroxide monohydrate are provided in Fig.

5. All of the peaks observed in the Raman spectra of lithium hydroxide monohydrate have been previously identified in the literature.²² Peak assignments and observed isotopic shifts are provided in Table 3. Four new isotopic shifts in the Raman spectrum of lithium carbonate have been identified.

Nine peaks were observed in the Raman spectrum of lithium hydroxide monohydrate in this work that match the literature. The five low frequency Raman bands observed below 300 cm⁻¹ are assigned to translational vibrations of OH and H₂O groups in the lattice structure.²² Four of these bands exhibit very slight isotopic shifts (on the order of 1 cm⁻¹) upon substitution of the lithium isotope even though the lithium does not directly participate in the vibrations (see Fig. 5A). Isotopic shifts observed in the Raman bands arising from these lattice vibrations have not been reported in the literature to date. Three peaks in the middle frequency region of the spectrum are attributed to translational vibrations of the lithium atoms in the lattice and exhibit significant frequency shifts (up to 25 cm⁻¹) upon substitution of the lithium isotope, as seen in Fig. 5B. The isotopic shifts of the lithium lattice translations have been previously reported in the literature.²² A slight isotopic shift of the Raman band near 850 cm⁻¹, assigned to a rotational lattice vibration of H₂O, is shown in Fig. 5C. Hase also reported the band at 850 cm⁻¹ in the Raman spectrum of lithium hydroxide monohydrate spectrum and attributed the shift of this band to the lithium isotope substitution.²² Similarly, the Raman band which is located at a longer wavelength

is relatively weak and noisy. Parts of the spectra which contain this band were smoothed with a five point rolling average and then fit with Voigt profiles. The resulting new forms of the spectra are presented in Fig. 6. The calculated Voigt profiles match the shape of the Raman band at 850 cm⁻¹ well, and exhibit an isotopic shift of approximately 3 cm⁻¹.

[Insert Figure 5]

[Insert Figure 6]

Table 3. The shifts observed in the Raman bands of lithium hydroxide monohydrate upon substitution of ⁶Li and ⁷Li isotopes. The band assignments are based on the literature.

Raman band locations (cm ⁻¹) ²²			Observed band locations and shifts (cm ⁻¹) in this work				Assignments to the lattice vibrations ²²
⁶ Li	⁷ Li	Strength	⁶ Li	⁷ Li	Shift / #pixels	Resolution per pixel	
86	86	M	92.50	92.27	0.23 / 1	0.22	OH/H2O translation
96	96	W	n.o.	n.o.	n.o.		OH/H2O translation
119	119	M	125.23	124.14	1.09 / 5	0.22	OH/H2O translation
145	145	S	149.92	150.03	-0.11 / < 1	0.21	OH/H2O translation
214	214	M	219.67	218.20	1.47 / 7	0.21	OH/H2O translation
248	248	M	251.14	250.42	0.72 / 3	0.20	OH/H2O translation
389	368	M	393.32	371.72	21.6 / 108	0.20	Li lattice translation
414	394	M	421.27	397.54	23.73 / 119	0.20	Li lattice translation
542	516	M	547.51	520.72	26.79 / 141	0.19	Li lattice translation
597	593	VW	n.o.	n.o.	n.o.		H2O rotation, B _g
703	696	W, br	n.o.	n.o.	n.o.		H2O rotation, B _g
842	841	m	847.44	844.04	3.4 / 20	0.17	H2O rotation, A _g

n.o. – not observed, S – strong, M – medium, W – weak, VW – very weak, br – broad

Principal Component Regression

Principal Component Regression was employed to determine the sensitivity of the Raman peak shifts of Li₂CO₃ to the isotopic composition of Lithium. Raman data from the ⁶Li and ⁷Li carbonate samples were digitally processed by convolving a second derivative gaussian filter (Sigma = 2wn, Range = 20wn).

$$\text{ProcessedSpec}(\varepsilon_k) = \sum_i [\text{RawSpec}(\varepsilon_i) * G''(\varepsilon_i - \varepsilon_k)]$$

$$G''(\varepsilon) = [(\sigma^2 - \varepsilon^2) / \sigma^4] * \text{Exp}(-\varepsilon^2 / (2\sigma^2))$$

$$\text{Where } \varepsilon_i \text{ is such that: } -10wn \leq (\varepsilon_i - \varepsilon_k) \leq 10wn$$

$$\text{And } \sigma = 2wn$$

The second derivative filter effectively suppresses broad background features and reduces noise. The processed Raman spectra were then individually normalized by scaling their root-mean-square (RMS) signal between 85wn and 215wn to 1.

$$\text{Norm_Factor} = \text{SquareRoot}[\sum_i [\text{ProcessedSpec}(\varepsilon_i)^2]]$$

Where ε_i is such that: $85\text{wn} \leq (\varepsilon_i) \leq 215\text{wn}$

$$\text{NormSpec}(\varepsilon_k) = \text{ProcessedSpec}(\varepsilon_k) / \text{Norm_Factor}$$

The normalized and processed spectra of ^6Li and ^7Li carbonate samples are shown in figure 7a.

[Insert Figure 7a,b]

Principal Component spectra were calculated from twenty Li_2CO_3 spectra, ten spectra from two locations of each of the 95 atom-% $^6\text{Li}_2\text{CO}_3$ and the 99 atom-% $^7\text{Li}_2\text{CO}_3$ materials. The result of the principal component analysis yielded two significant components, shown in figure 7b. The first principal component explains 95.75 % of the spectral set signal, the second explains 4.23%. Each additional component explains less than 0.006%.

A regression model was computed relating the two principal values, (which correspond to the scalar products of the two principal components with a normalized and processed Raman spectrum) to the ^6Li content.

$$^6\text{Li atom\%} = 603.156 - 567.344 * \text{PV1} - 228.634 * \text{PV2}$$

Where $\text{PV1} = \sum_i [\text{NormSpec}(\varepsilon_i) * \text{PC1}(\varepsilon_i)]$
and $\text{PV2} = \sum_i [\text{NormSpec}(\varepsilon_i) * \text{PC2}(\varepsilon_i)]$

The Principal Component Regression (PCR) model validation data set is composed of twenty Raman spectra from four additional samples made from blending ^6Li and ^7Li starting materials. Despite grinding and mixing, the blends were not a uniform composition and so predicted ^6Li content varied considerably from spot to spot on these materials. However, if the deviation from average of repeated measurements on any spot is compared, the results show a two-sigma standard deviation of 1.65 atom-%. Figure 8 shows the deviation from average for 40 spectra, 20 from the calibration set and 20 from the validation set. The model determined ^6Li atom-% is indicated by purple circles using the secondary axis on the righthand side of the chart.

[Insert Figure 8]

Conclusion

Isotopic analysis of lithium containing compounds is an essential area of research with applications in a wide variety of research areas including geochemistry and batteries. Currently there are limited field applicable experimental techniques capable of providing rapid analysis of lithium isotopes present in environmental samples. Raman spectroscopy is an ideal candidate for field applications, as it combines rugged and reliable experimental setups with non-destructive, standoff detection capabilities. In this work, isotopic shifts in Raman spectra due to substitution of the lithium isotope in lithium carbonate and lithium hydroxide monohydrate have been investigated. Building upon literature results of the Raman spectra of these two compounds, two new isotopic shifts were identified in the spectrum of lithium carbonate and four new isotopic shifts were identified in the spectrum of lithium hydroxide

monohydrate. This work also suggests that despite the small shifts of the major Raman lines, the isotopic content of Li carbonate material could be differentiated at a sensitivity level less than 2 atom% ^6Li .

Acknowledgements

This work was produced by Battelle Savannah River Alliance, LLC under Contract No.

89303321CEM000080 with the U.S. Department of Energy. Publisher acknowledges the U.S.

Government license to provide public access under the DOE Public Access Plan

(<http://energy.gov/downloads/doe-public-access-plan>). This work was supported by the Laboratory

Directed Research and Development (LDRD) program under project number LDRD-2021-00404 within the Savannah River National Laboratory (SRNL).

Competing Interests

The authors declare no competing or conflicting interests.

References

1. S.J. Fritz, T.M. Whitworth. "Hyperfiltration-induced fractionation of lithium isotopes: Ramifications relating to representativeness of aquifer sampling". *Water Resour. Res.* 1994. 30(2): 225-235.

<https://doi.org/10.1029/93WR02682>

2. H. Sun, Y. Gao, Y. Xiao, H. Gu, J.F. Casey. "Lithium isotope fractionation during incongruent melting: Constraints from post-collisional leucogranite and residual enclaves from Bengbu Uplift, China". *Chem. Geol.* 2016. 439: 71-82.

<https://doi.org/10.1016/j.chemgeo.2016.06.004>

3. S. Liu, Y. Li, J. Liu, Y. Ju, J. Liu, Z. Yang, Y., Shi. "Equilibrium lithium isotope fractionation in Li-bearing minerals". *Geochim. Cosmochim. Ac.* 2018. 235: 360-375. <https://doi.org/10.1016/j.gca.2018.05.029>

4. R. Millot, Ph. Négrel, E. Petelet-Giraud. "Multi-isotopic (Li, B, Sr, Nd) approach for geothermal reservoir characterization in the Limagne Basin (Massif Central, France)". *Appl. Geochem.* 2007. 22: 2307-2325. <https://doi.org/10.1016/j.apgeochem.2007.04.022>
5. W. Li, X. Liu, K. Wang, P. Koefoed. "Lithium and potassium isotope fractionation during silicate rock dissolution: An experimental approach". *Chem. Geol.* 2021. 568: 120142. <https://doi.org/10.1016/j.chemgeo.2021.120142>
6. L. Chan, J.M. Edmond. "Variation of lithium isotope composition in the marine environment: A preliminary report". *Geochim. Cosmochim. Ac.* 1988. 52(6): 1711-1717. [https://doi.org/10.1016/0016-7037\(88\)90239-6](https://doi.org/10.1016/0016-7037(88)90239-6)
7. Y. Takami, S. Yanase, T. Oi. "Observation of lithium isotope effects accompanying electrochemical release from lithium cobalt oxide". *Z. Naturforsch.* 2013. 68a: 73-78. <https://doi.org/10.5560/zna.2012-0080>
8. K. Okano, Y. Takami, S. Yanase, T. Oi. "Lithium isotope effects upon electrochemical release from lithium manganese oxide". *Energy. Proced.* 2015. 71: 140-148. <https://doi.org/10.1016/j.egypro.2014.11.864>
9. S. Yanase, W. Hayama, T. Oi. "Lithium isotope effect accompanying electrochemical intercalation of lithium into graphite". *Z. Naturforsch.* 2003. 58a: 306-312. <https://doi.org/10.1515/zna-2003-5-610>
10. H.P. Qi, T.B. Coplen, Q.Zh. Wand, Y.H. Wang. "Unnatural isotopic composition of lithium reagents". *Anal. Chem.* 1997. 69: 4076-4078. <https://doi.org/10.1021/ac9704669>
11. D.A. Cremers, A. Beddingfield, R. Smithwick, R.C. Chinni, C.R. Jones, B. Beardsley, L. Karch. "Monitoring uranium, hydrogen, and lithium and their isotopes using a compact laser-induced

- breakdown spectroscopy (LIBS) probe and high-resolution spectrometer". *Appl. Spectrosc.* 2012. 66(3): 250-261. <https://doi.org/10.1366%2F11-06314>
12. J.D. Ingle, Jr., S.R. Crouch. *Spectrochemical Analysis*, Prentice-Hall, New Jersey, 1988.
13. Y. Hase, I.V.P. Yoshida. "The Raman active vibrational modes and isotopic effects of four isotopically substituted lithium hydroxides". *Chem. Phys. Lett.* 1979. 65(1): 46-49. [https://doi.org/10.1016/0009-2614\(79\)80122-0](https://doi.org/10.1016/0009-2614(79)80122-0)
14. V.S. Gorelik, D. Bi, Y.P. Voinov., A.I. Vodchits, B.P. Gorshunov, N.I. Yurasov, I.I. Yurasova. "Raman spectra of lithium compounds". *J. Phys.: Conf. Ser.* 2017. 918: 012035. <https://doi.org/10.1088/1742-6596/918/1/012035>
15. V.I. Tyutyunnik. "Lithium hydroxide monohydrate single crystals: infrared reflectivity and Raman study". *J. Raman Spectrosc.* 2000. 31: 559-563. [https://doi.org/10.1002/1097-4555\(200007\)31:7%3C559::AID-JRS577%3E3.0.CO;2-O](https://doi.org/10.1002/1097-4555(200007)31:7%3C559::AID-JRS577%3E3.0.CO;2-O)
16. Y. Ishii, T. Nagasake, N. Igawa, H. Watanabe, H. Ohno. "Temperature dependence of the Raman spectrum in lithium oxide single crystal". *J. Am. Ceram. Soc.* 1991. 74(9): 2324-2326. <https://doi.org/10.1111/j.1151-2916.1991.tb08308.x>
17. M.H. Brooker, J.B. Bates. "Raman and infrared spectral studies of anhydrous Li_2CO_3 and Na_2CO_3 ". *J. Chem. Phys.* 1971. 54: 4788-4796. <https://doi.org/10.1063/1.1674754>
18. M.H. Brooker, J. Wang. "Raman and infrared studies of lithium and cesium carbonates". *Spectrochim. Acta.* 1992. 48A(7): 999-1008. [https://doi.org/10.1016/0584-8539\(92\)80176-W](https://doi.org/10.1016/0584-8539(92)80176-W)
19. A. Anderson, F. Lüty. "Raman scattering, defect luminescence, and phonon spectra of ^7LiH , ^6LiH , and ^7LiD crystals". *Phys Rev. B.* 1983. 28(6): 3415-3421. <https://doi.org/10.1103/PhysRevB.28.3415>

20. Y. Hase, I.V.P. Yoshida. "Low frequency bands of Li_2CO_3 crystal". Spectrochim. Acta. 1979. 35A: 379.
[https://doi.org/10.1016/0584-8539\(79\)80196-8](https://doi.org/10.1016/0584-8539(79)80196-8)
21. Y. Hase, I.V.P. Yoshida. "Li-O Raman bands of $^6\text{Li}_2\text{CO}_3$ and $^7\text{Li}_2\text{CO}_3$ ". Spectrochim. Acta. 1979. 35A: 377-378. [https://doi.org/10.1016/0584-8539\(79\)80195-6](https://doi.org/10.1016/0584-8539(79)80195-6)
22. Y. Hase. "Raman spectroscopic study of four isotopically substituted lithium hydroxide monohydrates". Monatshefte fur Chemie. 1981. 112: 73-82. <https://doi.org/10.1007/BF00906244>
23. L.B. Breitenfeld, M.D. Dyar, C.J. Carey, T.J. Tague Jr., P. Wang, T. Mullen, M. Parente. "Predicting olivine composition using Raman spectroscopy through band shift and multivariate analyses". Am. Mineral. 2018. 103(11): 1827-1836. <https://doi.org/10.2138/am-2018-6291>
24. A. Chopelas. "Single crystal Raman spectra of forsterite, fayalite, and monticellite". Am. Mineral. 1991. 76: 1101-1109.

Figures

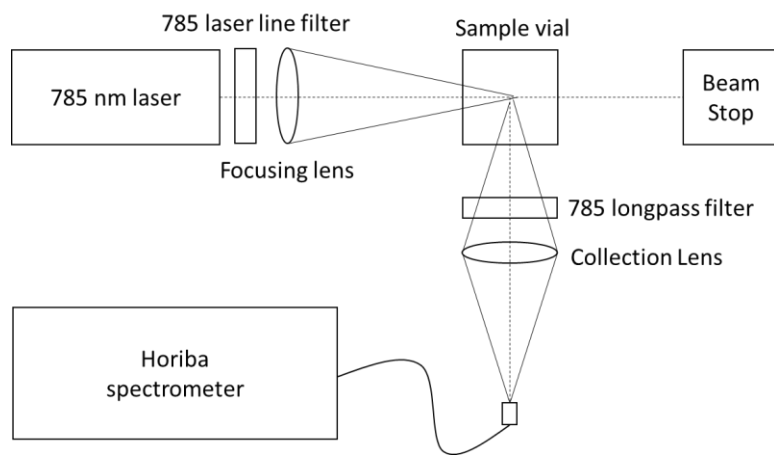


Fig. 1. A block diagram of the experimental setup used for Raman measurements.

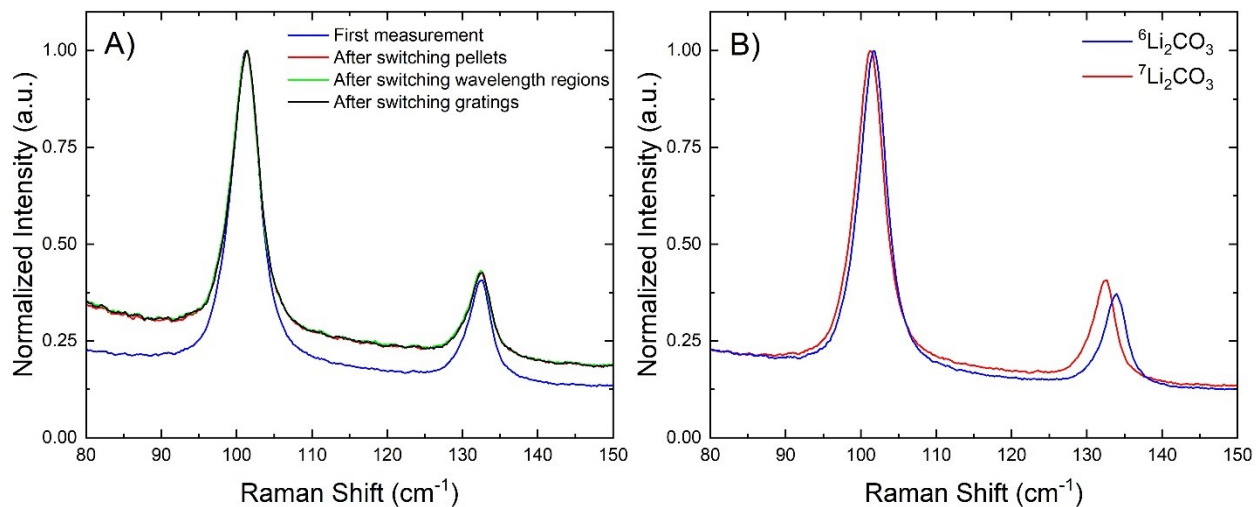


Fig. 2. Comparisons for two bands observed around 101 and 131 cm⁻¹ in the Raman spectra of Li₂CO₃. A) the locations of the two bands in the Raman spectra of ⁷Li₂CO₃ after moving spectrometer parts and switching sample pellets, B) the locations of the two bands in both ⁶Li₂CO₃ and ⁷Li₂CO₃.

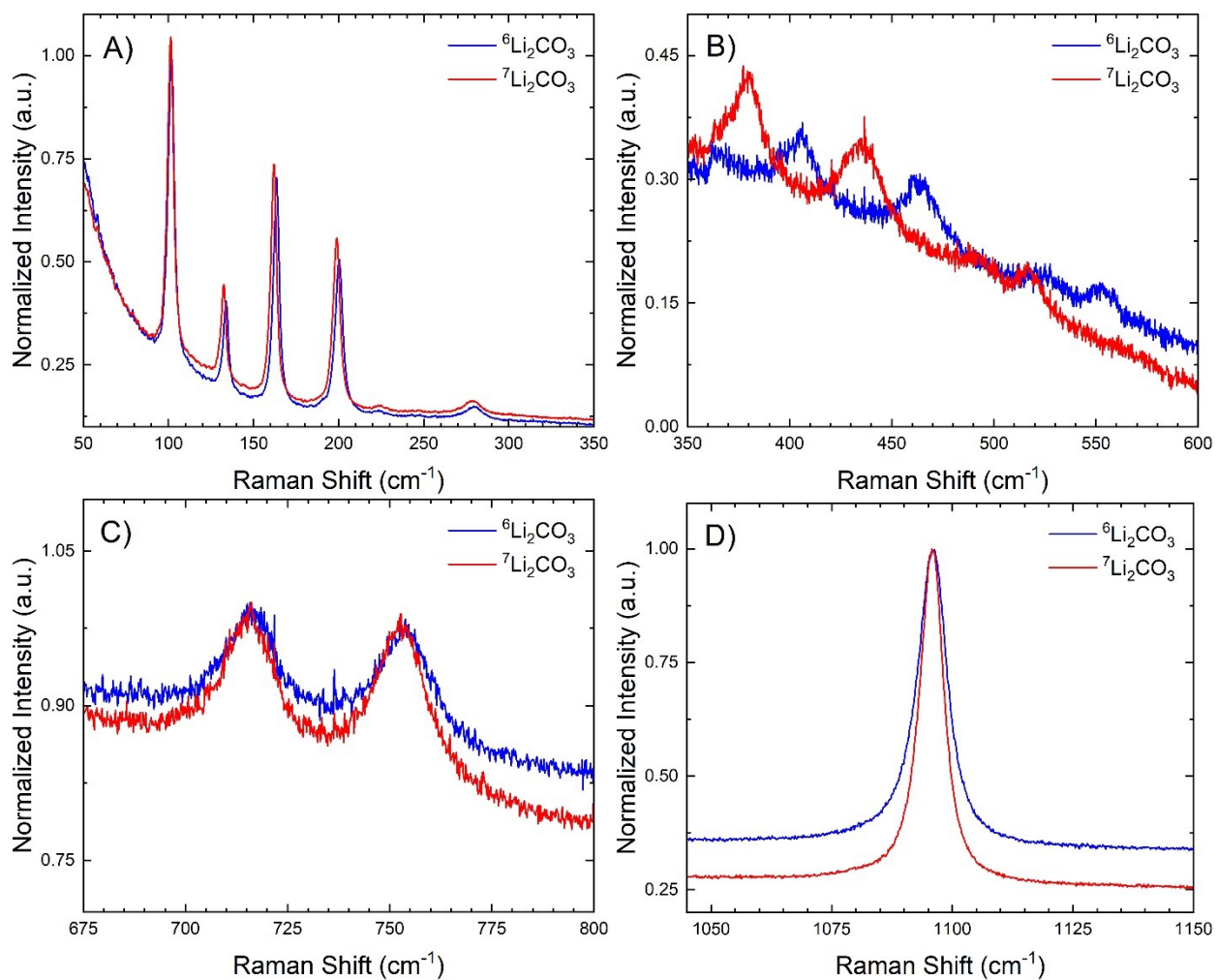


Fig. 3. Comparison of the bands observed in the Raman spectra of ${}^6\text{Li}_2\text{CO}_3$ (blue) and ${}^7\text{Li}_2\text{CO}_3$ (red). A) Rotational and translational vibrations of the CO_3 lattice structure, B) translational vibrations of Li-O bonds, C) ν_4 fundamental vibrations of the CO_3 moiety, D) symmetric stretching vibration of the CO_3 moiety.

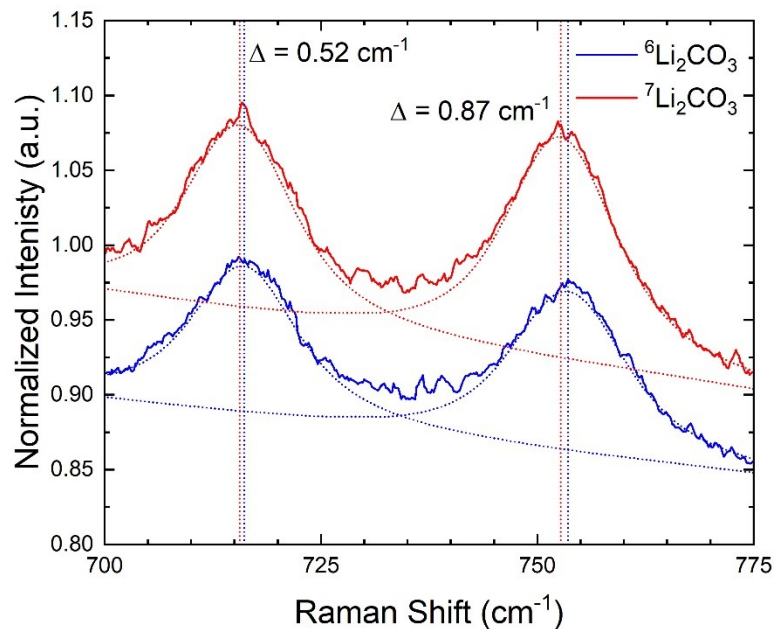


Fig. 4. The smoothing operation applied to the noisy peaks examined in the Raman spectra of ${}^6\text{Li}_2\text{CO}_3$ (blue) and ${}^7\text{Li}_2\text{CO}_3$ (red). The spectra are vertically displaced for clarity. The dashed lines correspond to the Voigt profiles fitting each peak and the peak centers are indicated by vertical dashed lines.

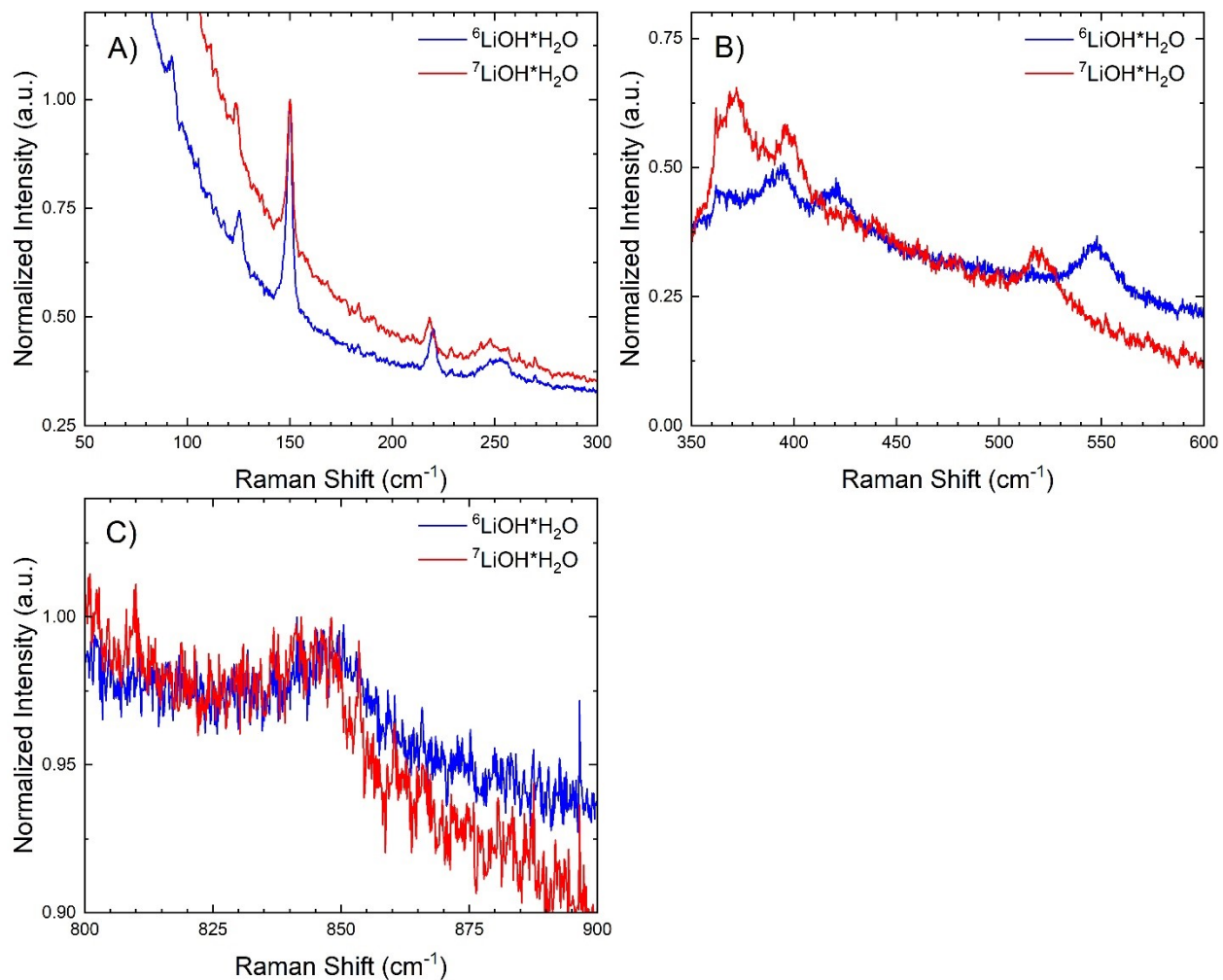


Fig. 5. Comparison of the bands observed in the Raman spectra of ${}^6\text{LiOH}\cdot\text{H}_2\text{O}$ (blue) and ${}^7\text{LiOH}\cdot\text{H}_2\text{O}$ (red). A) Translational vibrations of OH and H_2O groups in the lattice structure, B) translational vibrations of lithium atoms in the lattice structure, and C) rotational lattice vibration of H_2O

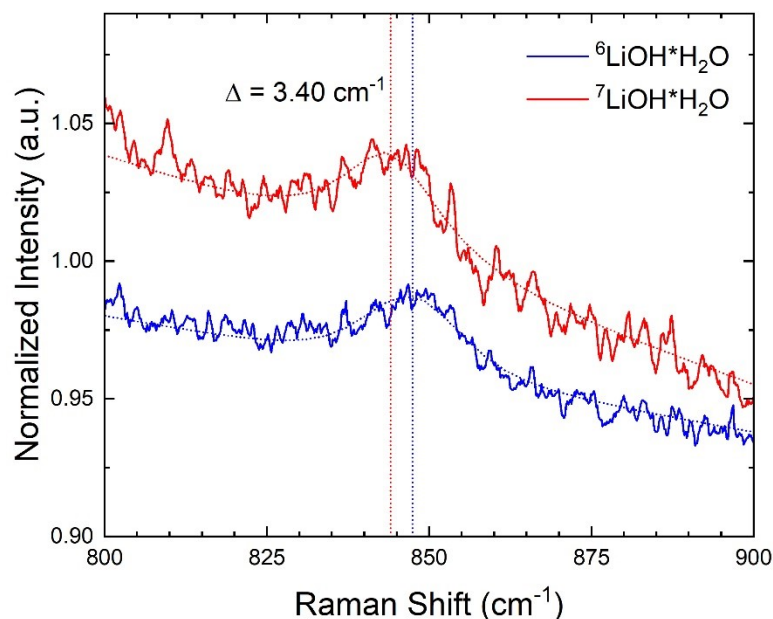


Fig. 6. The smoothing operation applied to the noisy peaks examined in the Raman spectra of ⁶LiOH·H₂O (blue) and ⁷LiOH·H₂O (red). The spectra are vertically displaced for clarity. The dashed lines correspond to the Voigt profiles fitting each peak and the peak centers are indicated by vertical dashed lines.

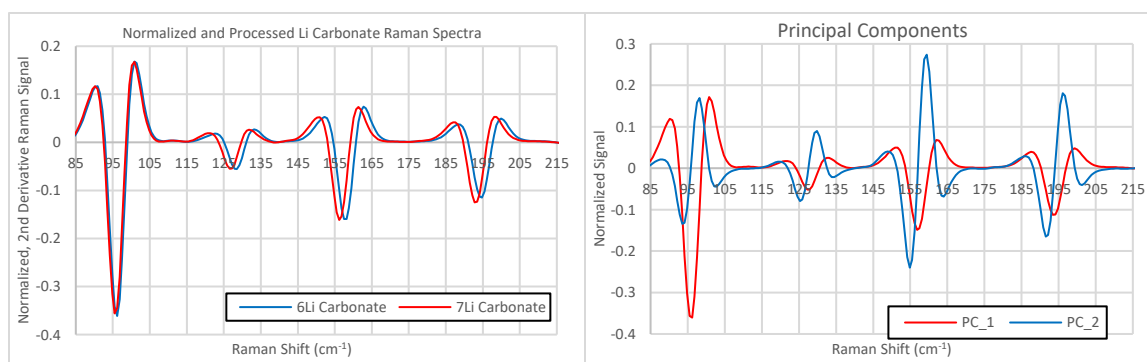


Fig. 7 Processed Raman Spectra and Principal Components. A) Second-derivative-processed and normalized Raman spectra of 95 atom% ⁶Li₂CO₃ (blue trace) and 99 atom% ⁷Li₂CO₃ (red trace). B) Principal Components calculated from ⁶Li₂CO₃ and ⁷Li₂CO₃ Raman spectra. PC_1 is the red trace, PC_2 is the blue trace.

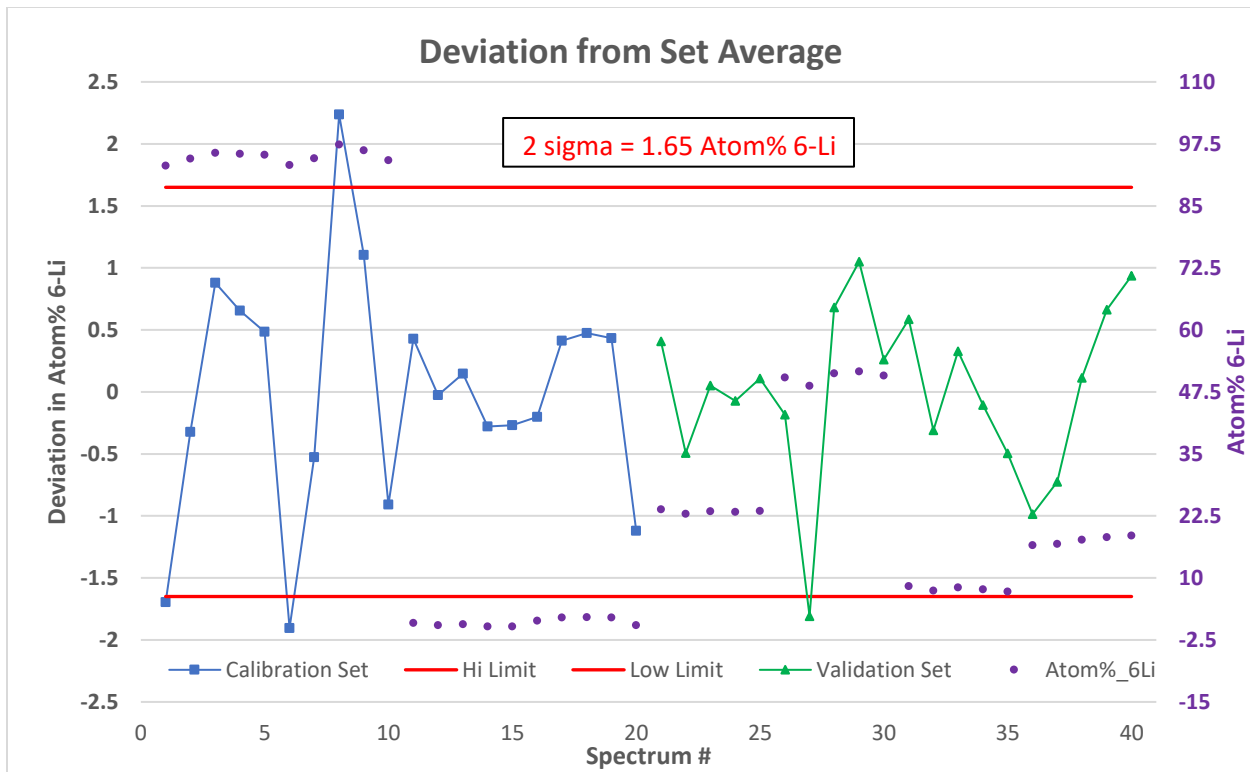


Fig. 8. Deviation from the PCR-model-predicted average ${}^6\text{Li}$ content of six Li_2CO_3 samples. The blue curve shows deviation of the two samples used in the calibration data set. The green curve shows deviation of the four samples in the validation data set. The red lines indicate the 2-sigma standard deviation of all 40 samples. The purple circles show the PCR-model-predicted average ${}^6\text{Li}$ content of the six samples using the secondary y-axis on the righthand side of the chart.

APPENDIX:

Responses to Reviewers

Reviewer 1:

The concerns raised by reviewer 1 are focused on the practicality of using Raman spectroscopy to isotope ratios in real materials. This argument is based largely on three problems, outlined in detail below, two of which were taken into consideration in this revised submission of the manuscript.

Problem 1: Measuring Li isotopes in a mixture or real sample. The reviewer states “in materials where Li is not the dominant cation, or one of many, the intensity of these bands would be lower and therefore even more difficult to resolve with accuracy. The largest natural difference would also already be close to the resolution capabilities and anything lower would not be resolvable.”

Correction: Added the following disclaimer at the end of the introduction.

While this manuscript is largely focused on the identification of new isotopic shifts in the spectra of pure Li_2CO_3 and $\text{LiOH}\cdot\text{H}_2\text{O}$, it is important to note that real samples or mixtures would likely contain a significantly lower amount of lithium compounds. Thus a sample purification or extraction step would be necessary to accurately determine the isotope ratios in real samples using Raman spectroscopy, which traditionally struggles with sensitivity.

Problem 2: ability to measure peak shifts limit sensitivity. The reviewer states “if we also assume that there is a linear relationship between the isotopic content and the Raman band shift (i.e. obeys Vergard's law, which has been called into question recently for isotope substitution in vibrational spectroscopy: Xu et al. 2018 RSC Advances, 8, pp. 33985) then the most sensitive bands to isotope substitution reported, the 520 cm^{-1} band in $7\text{LiOH}\cdot\text{H}_2\text{O}$ and 517 cm^{-1} band in $7\text{Li}_2\text{CO}_3$, would shift by only 3.2 and 4.2 cm^{-1} for a 12% enrichment, respectively.”

Correction: This concern raised by the reviewer is both valid and important, and was addressed by the addition of a new subheading, additional discussion, and two new figures at the end of the results section involving the use of principal component analysis (PCA) of the four bands near 100 cm^{-1} in Li_2CO_3 to estimate ^6Li content in mixtures of $^6\text{Li}_2\text{CO}_3$ and $^7\text{Li}_2\text{CO}_3$ powder. This new section details the use of the 3 peaks that shift on the order of $1\text{-}2\text{ cm}^{-1}$ between 95% ^6Li and 1% ^6Li to estimate ^6Li content. While Vergard's Law can serve as a useful approximation when estimating peak shifts due to isotopic substitution where shifts are small in comparison to peak widths, a more proper way for determining peak shift is spectral decomposition. Careful background correction and analysis result in a sensitivity to changes in the ^6Li concentration of below 2% when using 532 nm excitation. For example, this method could be used to distinguish samples containing 10% and 12% ^6Li , even though the peaks individually are only shifting by $\sim 2\text{ cm}^{-1}$ when going from 95% to 1% ^6Li . This sensitivity to the change in ^6Li is improved further to $\sim 1\%$ when changing the excitation wavelength from 532 nm to 785 nm.

Problem 3: crystal orientation could account for the small shifts observed

Rebuttal: Shifts due to orientation would be observable in measurements on single crystals, but because our experiments used pressed powder pellets of many randomly oriented crystals, these single crystal orientation effects will not be seen. These results in Raman spectroscopy are similar to the differences

between single-crystal and powder x-ray diffraction. No changes to the manuscript were made in response to this point.

Reviewer 2:

The only concern raised by this reviewer involves the assignment of the Li-O bands that are shifting significantly upon substitution of the Li isotope, specifically the broad bands in the 400-600 cm^{-1} range for both the carbonate and hydroxide. The reviewer states that the expected frequency ratio calculated using the reduced masses of the interaction and the force constant (assuming $^6\text{Li-O}$ and $^7\text{Li-O}$ have the same force constant, which is not true in practice, but a different force constant for these two bonds has not been found) should be 0.9449. This expected ratio assumes that the interaction is occurring undisturbed in space, which is not the case in practice either. The four peaks that we measured in lithium carbonate provided an average frequency ratio of approximately 0.9382, which is not identical to the experimental theoretical ratio, but is very close to the average frequency ratio in the original band assignment publication by Hase, in which the average frequency ratio is 0.9381. The experimental and literature results are in good agreement, and would likely match the theoretical ratio with proper determination of a different force constant for $^6\text{Li-O}$ and incorporation of effects of the larger crystal structure on these lattice vibrations.

Similar results hold for the three bands assigned to Li lattice vibrations in lithium hydroxide monohydrate, with experimental and literature results providing similar results, but not identical to the expected theoretical value.